Geomechanics and Engineering, *Vol. 32, No. 1 (2023) 97-110*
https://doi.org/10.12989/gae.2023.32.1.097

Measurement of K_0 and K_0' during loading and unloading of loose sand

Shay Nachum[a], Mark Talesnick[b] and Sam Frydman*

Faculty of Civil & Environmental Engineering, Technion – Israel Institute of Technology, Haifa, 32000, Israel

(*Received January 5, 2022, Revised October 24, 2022, Accepted December 24, 2022*)

Abstract. The coefficient of lateral earth pressure at rest in loose sand during virgin loading, K_0, and during unloading, K_0', have been determined from laterally confined load-unload tests. The tests included measurement of lateral pressure with null pressure gauges, side wall friction with newly designed friction meters and applied pressure and base pressure with load cells. The importance of accounting for side-wall friction when evaluating the distribution of vertical pressure over the height of the soil specimen was demonstrated. Relatively uniform friction was observed during loading, but this was not the case during unloading unless friction reduction measures were employed. While the measured value of K_0 was found to be close to, if slightly higher than the value commonly estimated on the basis of friction angle, φ', the ratio of K_0' to K_0 was found to reasonably fit an expression of the form $K_0'/K_0 = 1 + C \cdot \log(OCR)$, with C equal to 1 in the present tests.

Keywords: K_0; confined loading; confined unloading; loose sand; side-wall friction

1. Introduction

The coefficient of earth pressure at rest, K_0, has a significant effect on the initial stresses in the soil, and, consequently, on the changes in the stress and strain fields which develop during execution of geotechnical works. For example, Golpasand *et al.* (2018) found that different values of K_0 lead to opposite patterns of tunnel deformation during excavation. Consequently, a reasonable estimate of K_0 is necessary for a reasonable design estimate of structural response to changing in-situ conditions. Different approaches have been used to estimate K_0. In addition to direct, physical measurements, estimates have recently been made by employing numerical analyses using the discrete element method (DEM) (e.g. Gao and Wang 2014, Gu *et al.* 2015, Gu *et al.* 2018), and by interpreting results of common field tests (e.g. Hossain and Andrus 2016). However, the most common, and most reliable approach is still measurement in well controlled laboratory investigations. Issues influencing the laboratory determination of K_0 have been discussed, previously, by the authors (Talesnick 2012, Talesnick and Frydman 2019, Talesnick *et al.* 2020). In particular, it was demonstrated (Talesnick *et al.* 2020) that erroneous estimates may result from incorrect measurement of lateral soil pressure under an assumed condition of zero lateral movement, and from erroneous estimation of the vertical soil pressure adjacent to the location of lateral pressure measurement. The latter error often occurs in measurements performed in a rigid measuring cell, where the lateral pressure is measured on the side wall, and the associated vertical pressure is assumed equal to the pressure applied at the top of the cell. This assumption ignores friction along the cell wall, leading to an erroneous estimation of the vertical pressure.

Various methods have been used to measure lateral soil pressure under a laterally confined condition, but, as pointed out by Talesnick *et al.* (2020), these have generally not ensured absolute confinement, and, contrary to common belief, even extremely small lateral movement significantly affects the lateral soil pressure. In fact, measurement of soil pressure (not only lateral) by any sensor dependent on displacement/deformation (e.g., flexible diaphragm pressure cells) provides incorrect measurements, and although the resulting "cell effect" may be calibrated for loading in a particular soil at a particular initial condition, this is not realistically possible for various unload – reload stages.

Results of past experimental K_0 determinations, which were generally unaware of the above issues, have formed the basis for empirical expressions adopted universally for the estimation of K_0 under loading, unloading and reloading conditions. The most common of these is the following expression, an approximation to an expression originally developed theoretically by Jaky (1944) for virgin loading, based on the assumption that the soil is in a plastic, limit state

$$K_0 = 1 - sin\varphi' \tag{1}$$

where φ' is the effective angle of internal friction of the soil.

Jaky's assumption that K_0 loading represents a plastic, limit state in the soil is clearly incorrect (e.g., Michalowski 2005). However, numerous researchers have claimed reasonable experimental agreement with Eq. (1) under test conditions where zero lateral movement was presumed and vertical stress was assumed to be known. It has achieved almost universal acceptance, and is used as a default

*Corresponding author, Emeritus Professor
E-mail: cvrsfsf@technion.ac.il
[a]Post-doctoral researcher
E-mail: shay3090@gmail.com
[b]Associate Pofessor
E-mail: talesnik@technion.ac.il

ISSN: 2005-307X (Print), 2092-6219 (Online)

estimate in many numerical calculation packages, such as Plaxis, for analysis of a variety of geotechnical works. For example, Plaxis analyses adopting this relationship were used recently by Mansouri and Asghari-Kalijahi (2019) for modeling the excavation of a Tabriz metro underground station, by Dehghanbanadaki *et al.* (2020) to model stabilization of fibrous peat by end-bearing cement deep mixing columns, by Boulfoul *et al.* (2020) for establishing the optimal location of a pile for slope stabilization, by Watcharasawe *et al.* (2021) to analyze load sharing in a pile-raft foundation, and by Yazici and Keskin (2021) for optimizing a multi-anchored sheet pile wall. The validity of Eq. (1) is never questioned, and the possibility that the soil is preloaded is generally not taken into account.

For unloading, Schmidt (1966) suggested that the coefficient, hereon designated as K_0', could be related to K_0 and the over-consolidation ratio, *OCR*, by an expression of the following form

$$K_0' = K_0 \cdot OCR^{\alpha} \tag{2}$$

Mayne and Kulhawy (1982), from a study of an extensive collection of experimental data, recommended that α be taken as $\sin\varphi'$, resulting in the proposed, empirical expression

$$K_0' = (1\text{-}\sin\varphi') \cdot OCR^{\sin\varphi'} \tag{3}$$

Eq. (3) has also become commonly accepted and has also been adopted in national standards and handbooks (e.g., CGS 2006; ISI 2008).

Talesnick *et al*. (2020) tested 30 mm high samples of sand and clay, vertically loaded and unloaded statically in a rigid, rectangular cell of cross-section 60 mm x 60 mm. Lateral soil pressure was measure by two null soil pressure gauges (Talesnick 2005) fixed flush at mid-height of the inner surfaces of two opposing cell side walls. The influence of sidewall friction was investigated by performing some of the tests using friction reduction measures (FRM) based on Tognon *et al.* (1999), and others without FRM. In all cases the overall friction on the sidewalls was determined as the difference between the load applied on the sample top, and that measured at the sample base. K_0 was estimated by dividing the measured horizontal pressure by the corresponding, adjacent vertical pressure calculated by assuming a linear variation from sample top to sample bottom. It was further assumed that K_0 and K_0' may be expressed as the ratio of horizontal to vertical pressure, regardless of friction on the sidewall. The investigation indicated that Eq. (3) does not satisfactorily estimate K_0' . It was demonstrated that for reliable determination, side-wall friction must be eliminated or taken into account when estimating the relevant vertical pressure.

This paper presents an extension of the above investigation. K_0 and K_0' of the above sand have been determined in a similar, but larger rigid rectangular cell, which allowed inclusion of five null soil pressure gauges and three newly designed wall friction gauges (Talesnick and Ringel 2020) over the sample height. These additional sensors provided information regarding the distribution of friction and both vertical and lateral stress over the sample height, allowing more reliable estimation of K_0 and K_0'. The validity of assuming a linear variation of the vertical stress between the sample top and base was investigated. Such an assumption, if valid, would facilitate testing with relatively accessible, standard commercial equipment, and negate the need for more complex measurement of sidewall friction.

2. Test setup and material

Experiments were performed in a prismatic aluminum cell with specimen cross-section of 120 mm by 120 mm (Fig. 1). The cell was designed in order to allow the following measurements under laterally confined conditions: (i) The vertical load applied to the specimen top, and that transferred to its base, (ii) The distribution of soil-wall friction along the specimen height, and (iii) The distribution of lateral soil pressure along the specimen height.

The square cross-section was selected to allow inclusion of planar soil pressure measurement gauges and friction meters flush with the test cell walls. The test cell is constructed of four interchangeable side walls each 200 mm in height, 152 mm in width and 32.3 mm in thickness. The cell base is square, 119.8 mm by 119.8 mm, with an overall thickness of 32.3 mm.

The cell was designed and constructed to be implemented in either floating or fixed wall configurations; only tests carried out in the floating wall configuration are considered here. In this configuration, the walls, which initially sit freely on the wall support (see Fig. 1), can translate vertically. During first loading, they cannot move downwards, despite the downward friction force of the compressing soil. However, during unloading they can move upwards with the rebounding soil, acting as floating walls.

The applied vertical force was monitored by a load cell mounted at the specimen top. The force divided by the contact area is hereafter referred to as the applied vertical pressure.

The specimen base pedestal was placed upon a second load cell, allowing the force reaching the specimen bottom to be measured (Fig. 1). This force divided by the base area is referred to as the base vertical pressure.

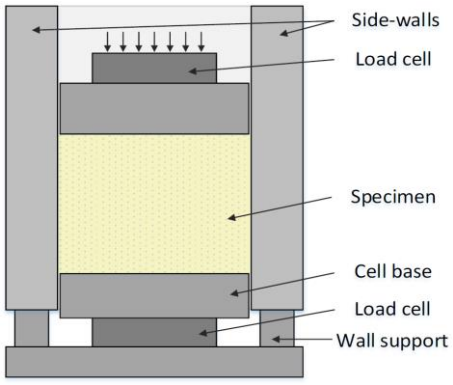

Fig. 1 Set-up of the test cell

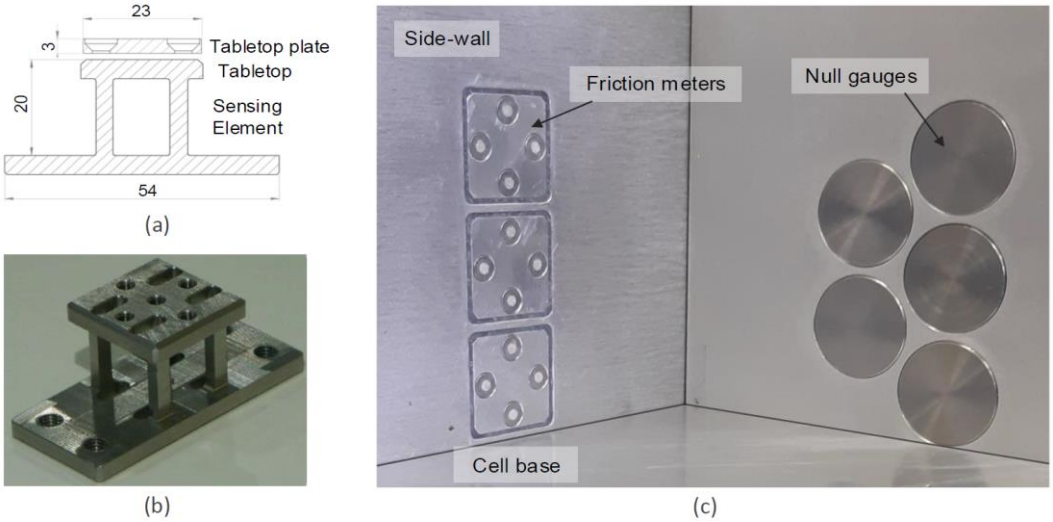

Fig. 2 Friction-meter (a) Schematic design (units in mm), (b) Photo and (c) Photo of the test cell

When a specimen is loaded vertically, the difference between the force applied on the upper surface of the specimen and that registered at its base represents the total vertical frictional load developed on the sidewalls of the cell.

The friction distribution along the wall was measured locally by an array of three friction-meters (Talesnick and Ringel 2020) mounted flush with the inner surface of one side wall at three different heights. The friction-meter sensing element is a monolithic, stainless steel, four-legged table (Figs. 2(a) and 2(b)).

The four legs respond to shear load applied to the "table-top" plate element (23 mm by 23 mm) which is fastened to the top of the sensing element and is located flush with the inner surface of the cell side wall. A clearance of 0.5 mm is left around all sides of the table-top plate relative to the cell wall; the face of the clearance is filled with silicon rubber (M-Coat C) which is cut flush with the inner surface of the cell side wall. The silicon rubber prevents sand from entering the clearance between the wall and the table-top plate, and, at the same time allows free deflection of the sensing element.

Lateral soil pressures were measured using an array of five Null Soil Pressure Gauges. The reliability of these gauges has been demonstrated previously (e.g., Talesnick 2005, Talesnick 2012, Talesnick *et al*. 2014, Talesnick and Frydman 2019, Talesnick *et al*. 2020, Talesnick and Bolton 2020). The gauges were mounted flush with the inner surface of another side wall at five different heights, providing the distribution of horizontal soil pressure along the wall. The Null Soil Pressure Gauges maintain zero membrane deflection over their entire area including the sensing area and consequently, the cell effect, mentioned earlier, is eliminated. The gauges used have a sensing diameter of 13 mm, outer diameter of 25 mm, and a nominal diaphragm thickness of 0.3 mm. In the test configuration used, full scale pressure is limited to 700 kPa.

The layout of the friction meters and pressure gauges used in the initial test series described below is shown in Figs. 2(c) and 3.

Two side wall friction conditions were considered. The default condition was that of the machine milled aluminum sidewalls. In the second condition, friction reduction measures (FRM) were applied based on Tognon *et al.* (1999), consisting of a polyethylene sheet (0.1 mm thick) with a thin layer of graphite grease. The grease was applied between the sheet and the side wall surface, allowing slippage between them. This method of friction reduction was considered superior to the application of lubricants which has been shown, for example, by Zheng *et al.* (2021) to be largely ineffective.

Specimens were statically compressed in the cell. Vertical load was applied to the specimen top through a rigid aluminum block at a rate of 28 kPa/min, and subsequently unloaded at the same rate. On average, a maximum vertical pressure of 300 kPa was applied to the specimen top. During load and unload, the vertical displacement of the specimen top was measured and the average vertical strain over the specimen height was calculated.

During unloading, as the walls tend to move upwards with the soil rebound, the motion of the walls was monitored at three corners of the cell with three LVDT's; the average of the three measurements is referred to as the wall heave during unload.

Sand specimens were tested. The sand tested is a fine, uniformly graded, quartz dune sand from Caesarea, classified as SP according to the Unified Soil Classification System (ASTM 2017). The mean grain size (D_{50}) is 0.25 mm (c_u= 1.7 and c_c=0.78), the specific gravity of the particles, G_s, is 2.68, and the minimum and maximum dry unit weights are 13.9 and 17.4 kN/m^3 respectively. The test specimens were prepared at a relative density, D_r= 34% by funneling dry sand grains into the test cell from a height of 10 mm (ASTM 2000). At this unit weight, the friction angle, φ, of the sand is about 33º (Frydman 2000).

In the initial test series, the specimen height was 93 mm - about the minimum height that allows insertion of all the

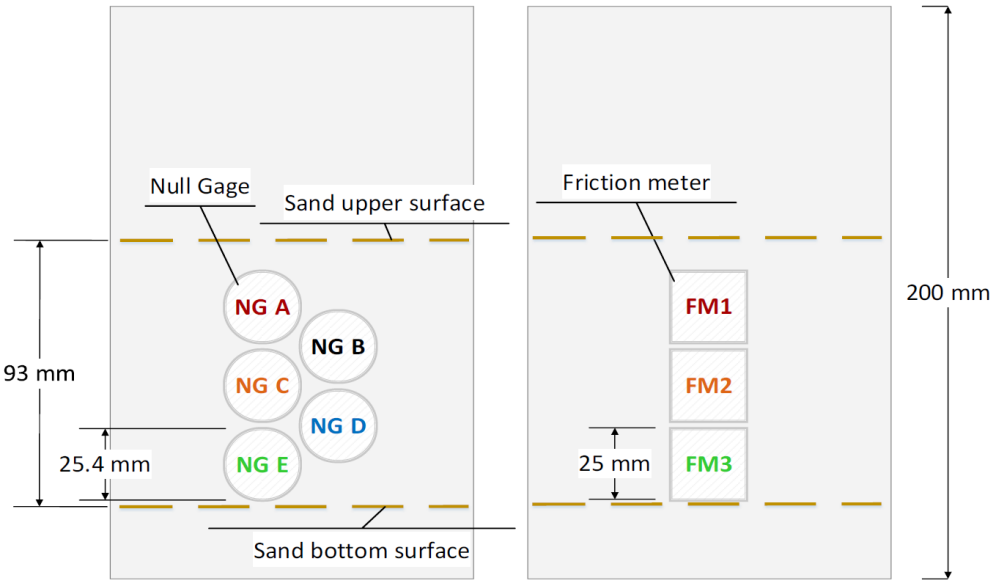

Fig. 3 Cell layout for 93 mm high specimen

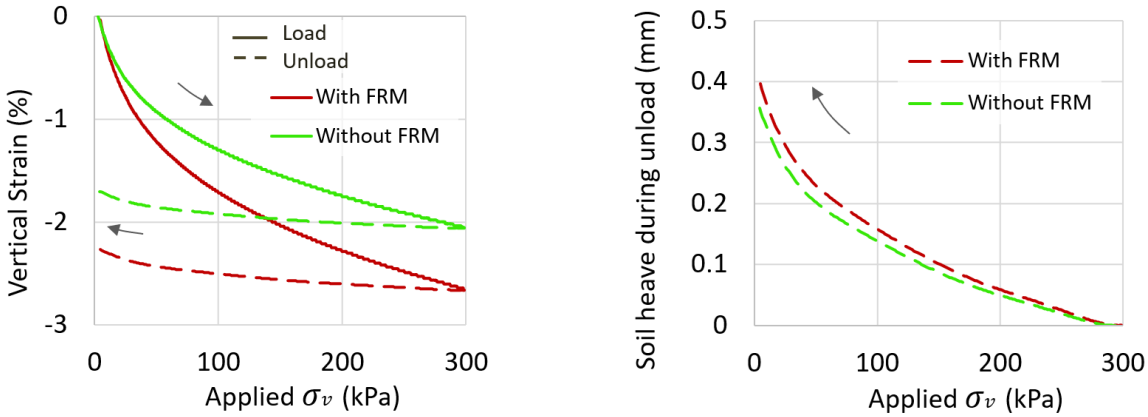

Fig. 4 Typical compression load-unload curve

gauges along the specimen's height. This height corresponds to a width to height ratio of 1.3.

3. Initial test series

3.1 Load-unload behavior

The influence of side-wall friction is illustrated by reference to the measured vertical deformation during a load-unload cycle as shown in Fig. 4. The unload curves are also shown in an expanded scale in Fig. 4.

The use of FRM results in the development of larger vertical strain under the same applied load – both compressional during loading and rebound during unloading.

The cell walls heave during unload as a function of the applied vertical pressure, as shown in Fig. 5. Comparing the soil movements (Fig. 4) to the wall movements (Fig. 5), it is clear that slip occurs between the soil and the wall from the start of unloading. As unloading advances, the influence of

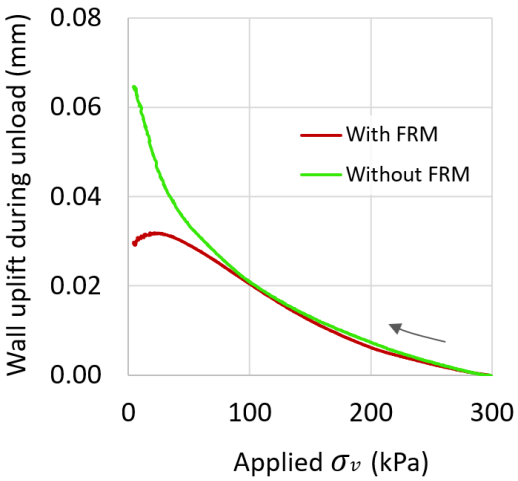

Fig. 5 Wall uplift during unloading

the FRM on the wall movement becomes apparent. The wall movement is similar over the first two thirds of the unloading, but the heave of the cell walls without FRM then

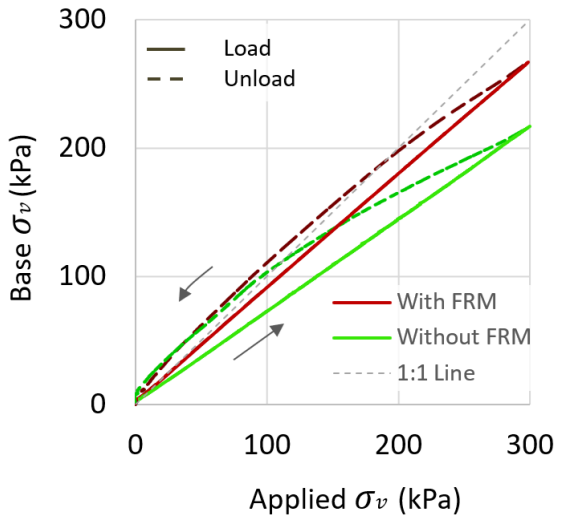

Fig. 6 Development of the base vertical pressure during loading and unloading

increases at an increasing rate, with friction opposing slip between the walls and the heaving soil. This friction is significantly reduced in the case with FRM and so the heaving soil partially slips along the walls, causing less wall uplift.

Side wall friction has a significant effect on the vertical and lateral distribution of vertical pressure within the specimen. Fig. 6 shows the development of the base vertical pressure as a function of the applied vertical pressure.

The plots indicate near-linear development of base vertical pressure as a function of the applied vertical pressure during loading. Note that when FRM are not employed, only about 75% of the applied vertical pressure reaches the specimen bottom. The use of FRM reduces side wall friction and consequently the load reaching the base of the specimen is approximately 90% of that applied to the specimen top.

During unloading, hysteresis is registered; the hysteresis is significantly greater in the test performed without FRM, and is a result of the reversal in direction of vertical frictional loads at the specimen sides as the specimen rebounds during unloading - the greater the friction the greater the hysteresis.

The difference between the force applied to the upper surface of the specimen and that registered at its base represents the total vertical frictional load developed on the sidewalls of the cell. The distribution of friction over the wall height is indicated by the friction values measured locally by the three friction-meters; the measurements during loading are shown in Fig. 7. Friction acting downwards on the soil and upwards on the wall is considered positive.

The use of FRM is clearly beneficial, reducing the friction to a third of that without FRM. The friction is almost uniform over the height of the wall, although the value near the base is slightly smaller.

In contrast to the relatively uniform distribution of friction during loading, the distribution during unloading is non-linear and non-uniform, as shown in Fig. 8.

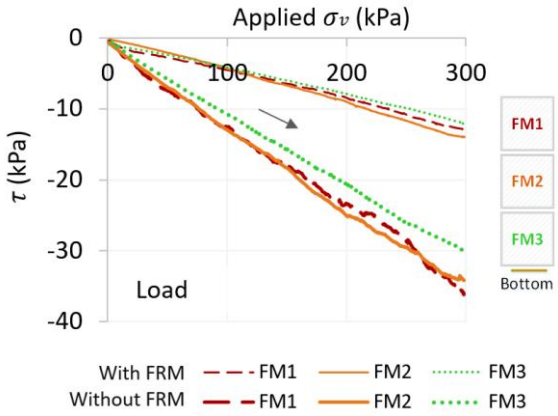

Fig. 7 Friction on sidewall during loading

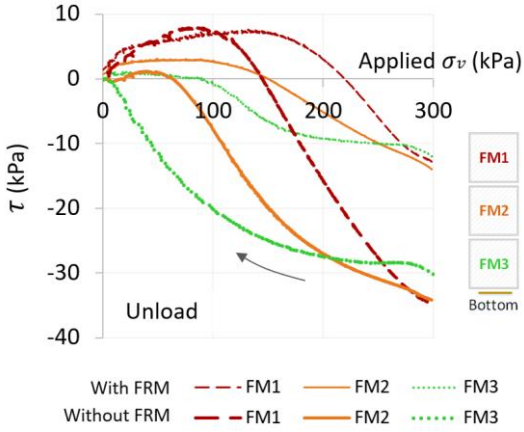

Fig. 8 Friction on sidewall during unloading

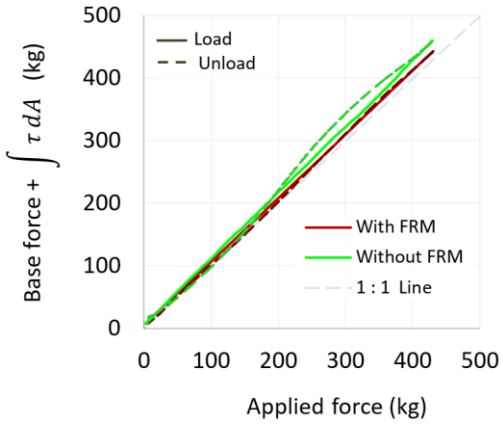

Fig. 9 Equilibrium check during loading and unloading

During unloading, the friction release occurs rapidly at the top of the specimen (FM1), with the rate decreasing downwards along the wall. Near the base of the specimen, little release of friction is evident until a third of the applied load has been removed. It appears that at the beginning of unloading (i.e. applied force decreasing at the top of the specimen), while the sand at the specimen top moves upwards, the sand near the base experiences little rebound and load release until a significant load decrease at the specimen top is completed. As unloading advances and sand rebounds upwards contrary to its previous downward

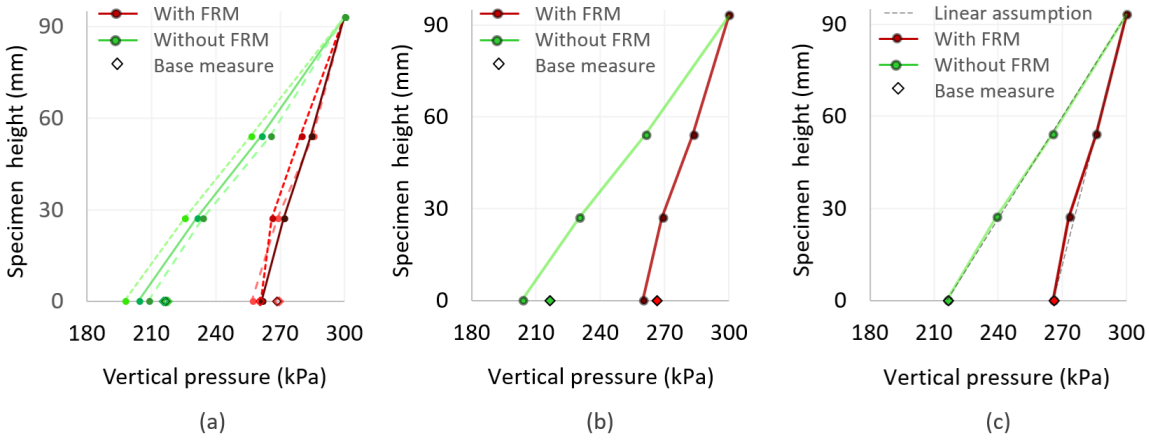

Fig. 10 Vertical pressure distribution during loading, from friction measurements along specimen wall, (a) individual tests; average, prior to adjustment and (c) following adjustment

movement during loading, the absolute friction force decreases, and eventually changes direction; this direction change occurs earliest and most extensively near the top of the specimen, later and less towards the base.

It can be seen that the FRM, which facilitate sand slip adjacent to the wall, influence both the magnitude of the friction and the shape of its distribution along the wall.

If the friction is assumed to be uniform across the width of the walls, the total friction force developed between the top and base of the specimen may be estimated by multiplying the integral of the frictional stress over the specimen height by the wall width and the number of walls (four). Fig. 9 shows an equilibrium check under these assumptions - the measured vertical base force summed together with the calculated total friction force plotted against the applied force.

When FRM are used, good agreement is observed, with less than 5% deviation during both loading and unloading. When FRM are not used, a deviation of slightly less than 10% is observed during loading, while a larger deviation and hysteresis are observed during unloading.

3.2 Distribution of vertical pressure over the specimen height

Evaluation of the coefficient of lateral earth pressure at rest requires definition of the horizontal and vertical soil pressures, σ'_h and σ'_v at the same location. The vertical pressure varies along the height of the specimen, and therefore adoption of the applied pressure, as is customarily done, may not, satisfactorily, represent the value which should be related to the horizontal pressure measured at a specific height for determination of K_0. The friction-meter readings indicate that the friction distribution during loading is nearly uniform (Fig. 7). Consequently, as a first approximation, it could be assumed that the vertical pressure varies linearly through the specimen height, from the applied vertical pressure at the specimen top to the base vertical pressure at the specimen bottom, allowing definition of a "representative" average vertical pressure at any particular height within the specimen. Since friction was measured by the three friction-meters placed along one wall, the measured values were used to estimate the actual vertical pressure distribution. Starting from the applied vertical pressure at the specimen top, the measured friction contributions were deducted down the specimen wall.

Fig. 10(a) shows the distribution of vertical pressure estimated in this way from three duplicate tests with both FRM and without FRM. The filled rhombi plotted at the base indicate the values of the measured base pressures for each test. The variations between the duplicate tests are seen to be extremely small, of the order of 3%, providing confidence with regards the reliability and repeatability of the sensing equipment and the test procedures. The difference between the measured and calculated base pressures is also small – up to about 5% in the case of tests performed with FRM and up to about 10% in tests performed without FRM. These deviations are probably a result of non-uniform friction over the widths of the specimen walls, and/or non-uniform distribution of the vertical pressure over the specimen area.

In view of the small variations in pressure distribution obtained from duplicate tests, average distributions, as well as average measured base pressures, are used for further calculations. The average distributions are shown in Fig. 10(b). In order to account for the difference between estimated and measured base pressures, the distribution in Fig. 10(b) has been corrected by proportionately distributing the difference up the wall, resulting in the adjusted distributions shown in Fig. 10(c).

Fig. 10 demonstrates that, as previously suggested, the pressure distribution over the specimen height during loading is approximately linear, regardless of whether FRM are applied or not. Consequently, as long as the load reaching the base is measured, it would be reasonable to assume a linear distribution of vertical pressure, and measurements of friction along the wall would not be required.

Whereas sidewall friction appears to be uniformly distributed along the specimen height during loading, this is not the case during unloading, as seen in Fig. 8. According to the measurements during unloading it cannot be assumed

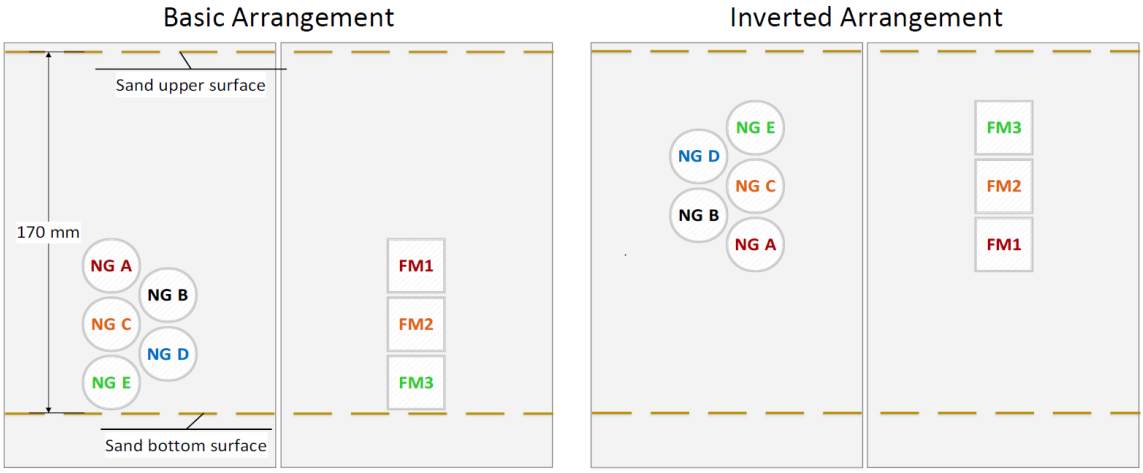

Fig. 11 Basic, and Inverted arrangements for testing of high specimens

that the vertical pressure varies linearly over the specimen height. It appears that determination of the vertical pressure along the specimen height needs to take account the distribution of friction and the base pressure measurement. In the present test setup, each friction meter covers about a third of the specimen height, and, in view of the non-linearity of the distribution of friction as shown in Fig. 8, the friction clearly varies, non-linearly, along each friction meter. Consequently, a reasonable distribution of vertical pressure cannot be obtained on the basis of the three friction meter measurements. As a result of this deficiency, a reliable distribution of vertical pressure and consequently, determination of K_0' could not be made during unloading from these measurements. It was recognized that a higher specimen would be required, allowing a larger number of friction measurements, in order to provide a reliable distribution of vertical pressure.

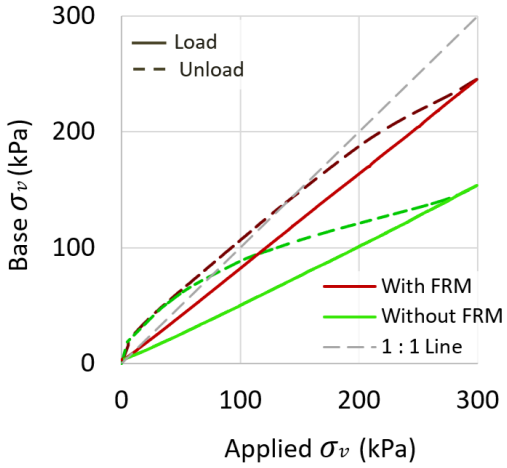

Fig. 12 Development of the soil base pressure in the high specimens during loading and unloading

4. Extended test series

4.1 Procedure for testing high specimens

Due to the limited size of the test cell and of the number and size of transducers available (5 null pressure gauges and 3 friction-meters), a novel approach was employed to investigate the distribution of vertical and horizontal pressures, and eventually of K_0 and K_0', over a greater specimen height of 170 mm. A series of specimens was prepared and tested according to the arrangement shown in Fig. 11, with the sensor arrays concentrated towards the specimen bottom ("Basic Arrangement"). A second series of specimens was prepared and tested with the cell inverted, such that the sensor arrays were concentrated in the upper portion of the specimen ("Inverted Arrangement"). Superposition of the measurements obtained from the two test conditions provided a full picture of the distribution of friction, vertical pressure and lateral pressure over the 170 mm height of the cell.

In the Basic Arrangement, three tests were performed without FRM and one with FRM; in the Inverted Arrangement, two tests were performed without FRM and three with FRM. In order to obtain a representative distribution of friction and lateral pressure along the entire specimen height for each wall condition (with or without FRM), the average distributions for the Basic and for the Inverted arrangements were first evaluated. The average distributions in the Inverted Arrangement were appended above the average distributions in the Basic Arrangement in order to estimate the distribution over the total height of the specimen. The average value of the sidewall friction at each friction-meter location was adopted for the determination of representative distributions of vertical pressure as a function of height within the specimen, in the same way as was applied for the regular specimens.

In view of the limitations of the tests performed in the initial series on the regular specimens, as discussed previously, only results of tests obtained from the high specimens were considered in studying the coefficient, K_0' during unloading.

4.2 Load-unload behavior

Tests were performed with and without FRM. Fig. 12

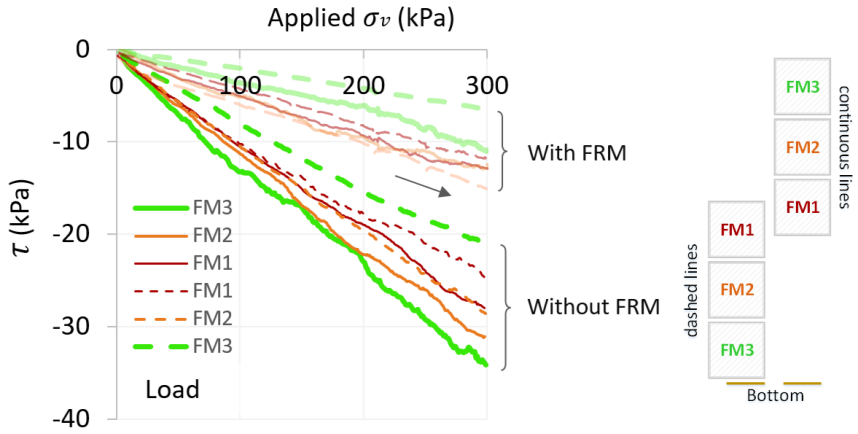

Fig. 13 Sidewall friction as a function of applied vertical pressure during loading, high specimens

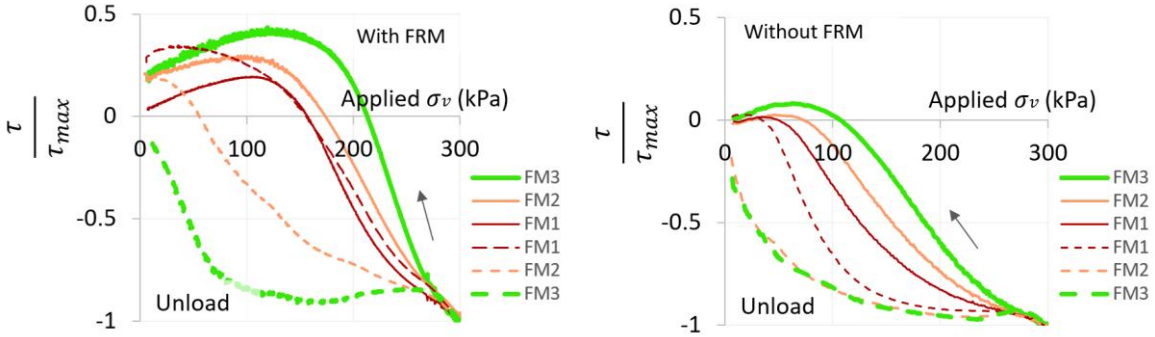

Fig. 14 Sidewall friction (normalized) as a function of applied vertical pressure during unloading, high specimens

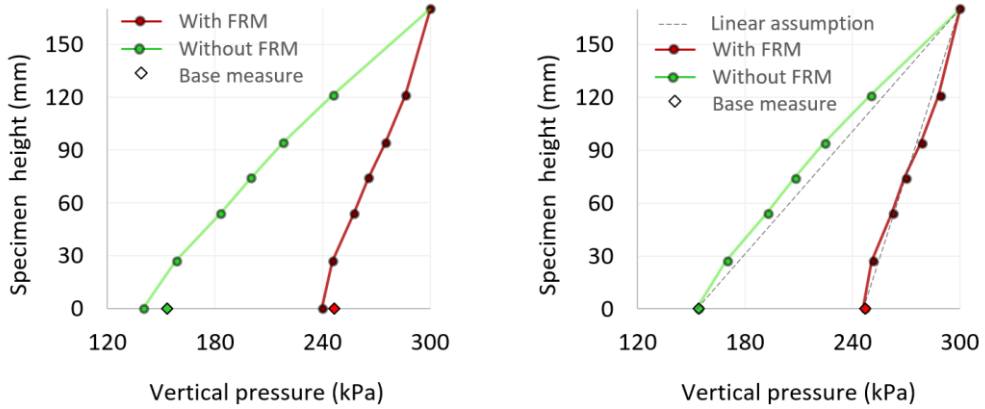

Fig. 15 Vertical pressure distribution during loading, from friction measurements along high specimen wall, (a) prior to adjustment and (b) following adjustment

shows a typical result of the development of the base vertical pressure as a function of the applied vertical pressure during loading and unloading. During loading, without FRM the base vertical pressure is only about 50% of the applied vertical pressure. In testing with FRM, pressure reaching the base is about 80% of the applied pressure.

Typical measurements of sidewall friction as a function of applied vertical pressure during loading are shown in Fig. 13, and during unloading in Fig. 14. Fig. 13 shows that the friction is less uniform than was obtained in the initial test series. Because of this non-uniformity, the unloading segment for each sensor begins from a different frictional value. To facilitate comparison between the unloading plots, each has been normalized by the friction at the end of the loading segment (Fig. 14).

The plots illustrate intuitive response of the measured friction. Friction is released rapidly at the specimen top where the applied vertical pressure is reduced. Consequently, the friction forces measured in the Inverted

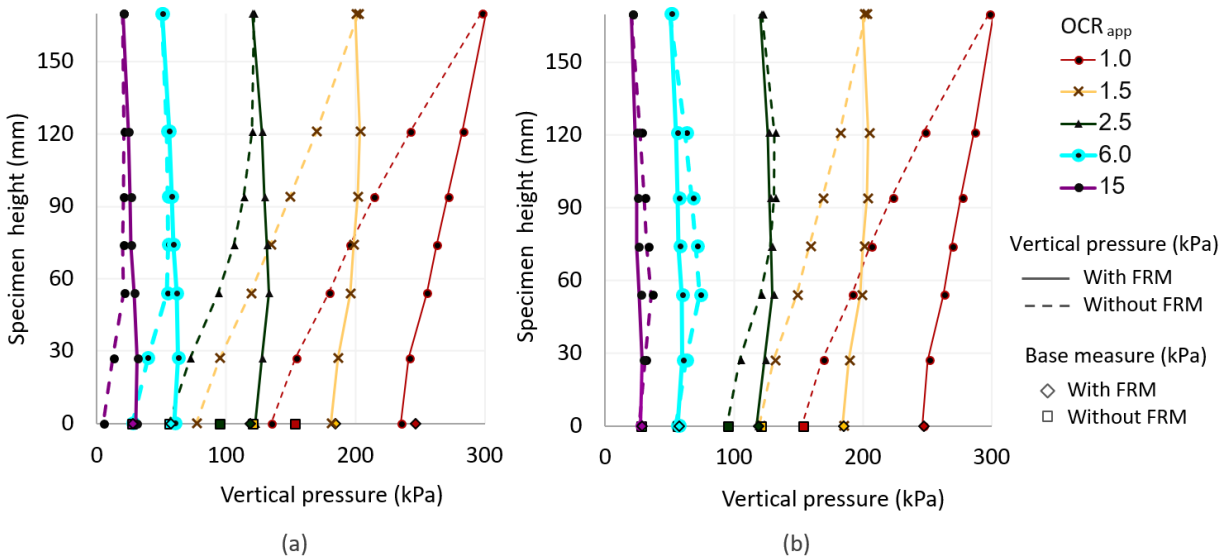

Fig. 16 Vertical pressure distribution during unloading, from friction measurements along high specimen wall, (a) prior to adjustment and (b) following adjustment

Arrangement have a greater tendency to change direction, from negative to positive, than those in the Basic Arrangement. As the applied vertical pressure approaches zero, reduction of friction in the lower part of the specimen occurs more rapidly. The order of the plots is consistent in both cases.

Distribution of vertical pressure along the specimen height has been calculated from the measured friction values, in a similar fashion to that used for the regular specimens. The resulting, average distributions, prior to and following adjustment (as in Fig. 10), are shown in Fig. 15 for loading, and Fig. 16 for unloading. Fig. 16 shows the vertical stress distributions as a function of $(OCR)_{app}$ - the overconsolidation ratio defined as the ratio of the maximum applied vertical pressure to the considered applied vertical pressure.

Fig. 16(a) shows the computed distribution of the vertical pressure (average over the area of the specimen) at the end of loading (OCR =1) and during unloading, for tests performed both with and without FRM. In the normally consolidated case, the discrepancy between the measured and calculated base pressure is small for both sidewall friction conditions.

However, in the cases where FRM were not used (dashed lines), the discrepancy between the measured base pressure and its calculated counterpart becomes larger as unloading proceeds and OCR increases. On the other hand, when FRM were used (solid lines), the discrepancy between the measured and calculated base pressure remains small also during unloading. When the pressure distributions are corrected to account for these discrepancies (Fig. 16(b)), and at higher values of OCR the differences for the two sidewall friction conditions decreases significantly and the distribution of vertical pressures tends to become more uniform along the specimen height. The plots of Figure 16b may be considered to reasonably represent the vertical pressure distribution with respect to elevation within the test cell.

4.3 K_0 during loading

Fig. 17 (regular specimens) and Fig. 18 (high specimens) show lateral pressure versus applied vertical pressure during loading, measured in the regular and high specimens respectively, with and without FRM. For the high specimens (Fig. 18), measurements from the B and D Null gauges are not shown, in order to present a clearer illustration of the data. The slope of any one plot could be interpreted as the coefficient of lateral earth pressure at rest (K_0), if the applied pressure was considered the relevant vertical pressure. The expressions included on the figures show the median and ranges of these K_0 for each condition. The plots illustrate the following characteristics:

- In all configurations, the measured horizontal pressure develops linearly with applied vertical pressure.
- In all configurations, the slopes of the plots decrease with depth of the point of lateral pressure measurement.
- The spread of the plots increases when FRM were not applied, and in the higher specimens relative to the regular specimens.

These observations would imply that K_0 is not a unique material parameter, but rather depends upon position of the measurement, sample height and/or frictional characteristics of the cell wall. This is, obviously, not a legitimate implication, and results from the fact that the lateral pressure measured at different locations along the wall height is divided by the vertical pressure applied at the top of the specimen rather than by a representative vertical pressure at the point of measurement of the lateral pressure.

A more rigorous approach to the problem is to estimate K_0 on the basis of the distributions of vertical pressure presented in Figs. 10 and 15(b) and of measured horizontal pressures presented in Figs. 17 and 18. Fig. 19 presents values of K_0 obtained using this approach for the tests on the regular and the high specimens, with and without FRM. K_0 has been determined separately based on the ratios

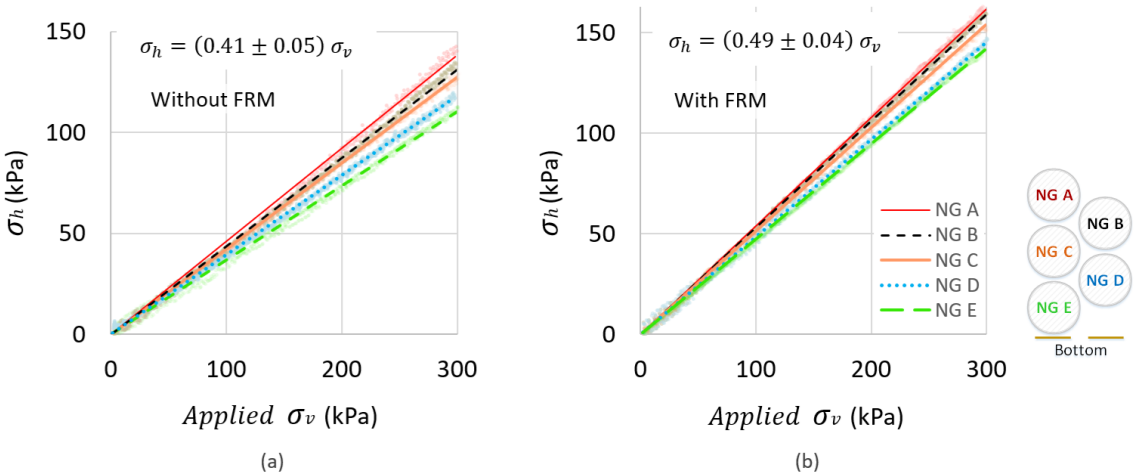

Fig. 17 Lateral pressure versus applied pressure, regular specimens, (a) no FRM and (b) with FRM

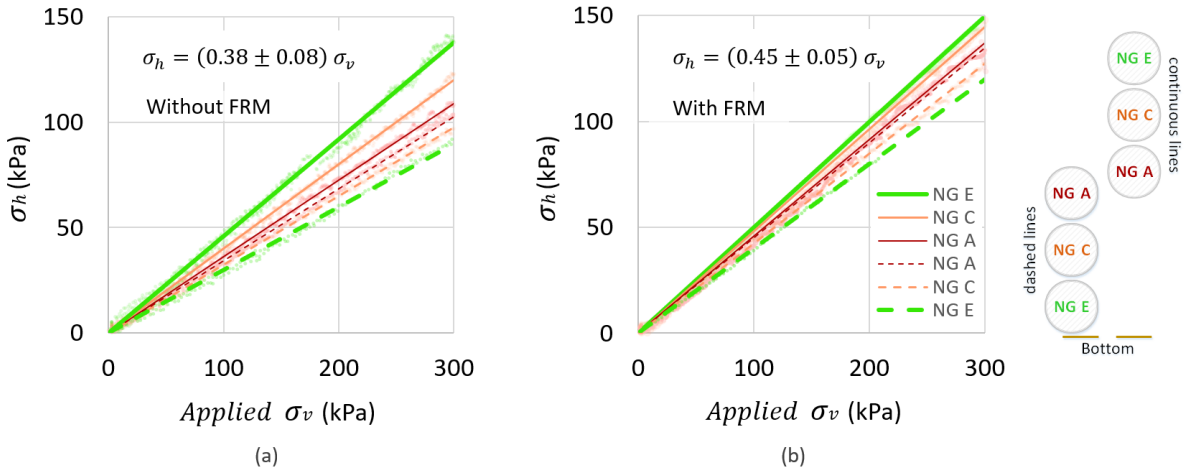

Fig. 18 Lateral pressure versus applied pressure, high specimens, (a) no FRM and (b) with FRM

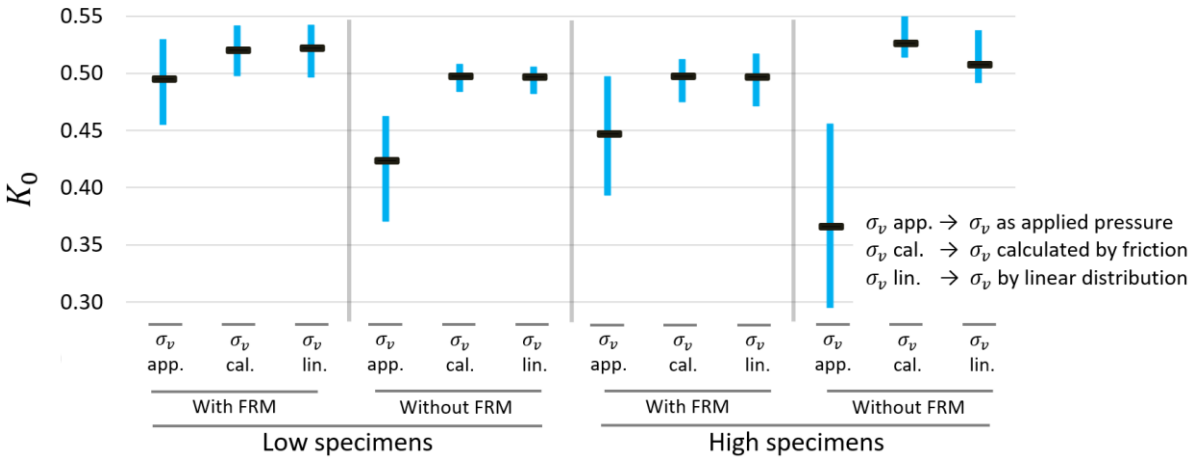

Fig. 19 Average and range of K_0 measured in regular and high specimens

between the measured horizontal pressures at the null gauge locations and three different estimations of the representative vertical pressures:

(a) the applied vertical pressure, (b) the vertical pressure at the null gauge location as calculated from the adjusted measured friction distribution, and (c) the vertical pressure at the null gauge location as obtained from an assumed linear distribution of vertical pressure from the measured values at specimen top and specimen bottom. Recognizing that K_0 should not depend on the location of

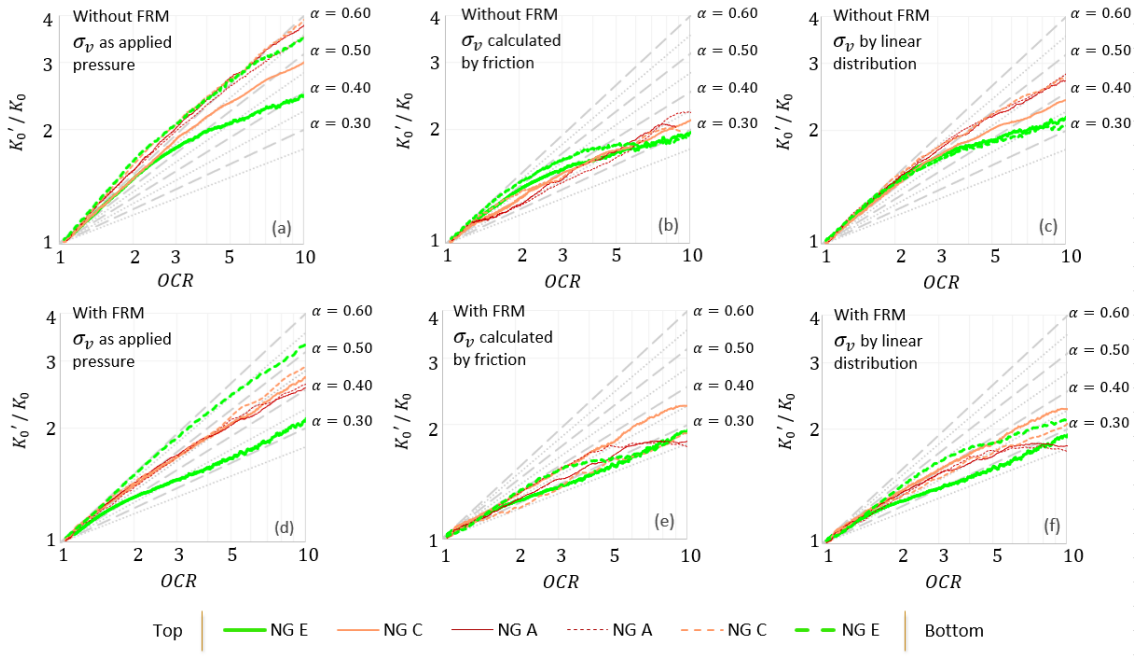

Fig. 20 K_0'/K_0 versus OCR; (a)-(c) without FRM; (d)-(f) with FRM

the measurement along the specimen, Fig. 19 shows the average, and range of values of K_0 over the specimen height for each of these three estimations, for each test condition.

Fig. 19 shows that the K_0 values based on the pressure applied at the specimen top are significantly and consistently lower than the others, and show larger variation over the specimen height. When the vertical pressure is estimated at the location of the horizontal pressure measurement, either from an assumed linear distribution or on the basis of friction measurements, more consistent values of K_0 result, with average values between 0.5 and 0.52 and ranges 0.47 – 0.54. When the vertical pressure is estimated by either of these two latter approaches, K_0 is seen to be reasonably independent of side wall friction conditions.

A significant conclusion from Fig. 19 is that during virgin loading, if a uniform distribution of friction is assumed, reasonable results are obtained, and there is no need for complex measurements of friction. It may be noted that according to prediction Eq. (1), adopting a value of φ' = 33º would lead to an estimated value of K_0 = 0.45, indicating an underestimate of about 11.5% relative to the average measured value of 0.51. This is consistent with tests carried out by Gao and Wang (2014) in which pressures were measured using tactile pressure sensors, and cell wall friction was largely eliminated, which indicated that Eq. (1) underestimated K_0 by about 11%.

4.4 K_0' during unloading

As explained above, only the high specimens were used for evaluation of K_0'. K_0' was calculated at each lateral pressure measurement location as the ratio of the measured lateral pressure to the adjacent vertical pressure. The latter was estimated by the three different approaches used for development of Fig. 19, i.e., by adopting the applied vertical pressure, by calculation down the wall based on measured friction, and by assuming a linear distribution between the known values at the specimen top and base. Fig. 20 shows log-log presentations of the development of K_0'/K_0 at null gauge locations as the overconsolidation ratio, OCR, increases during unloading. Figs. 20(a)-20(c) show the values for each of the vertical pressure estimation approaches for tests performed without FRM, and Figs. 20(d)-20(f) refer to tests performed with FRM. OCR is the overconsolidation ratio defined as the maximum vertical pressure, estimated at the null gauge location on completion of loading, divided by the estimated vertical pressure at that location at the specific unloading stage. The dashed, straight lines shown in Fig. 20 represent values of α, according to Eq. (2).

Referring to Fig. 20, several significant observations are apparent:

- In general, the test data at any location along the specimen wall does not fall along straight lines, so that it is not possible to define a distinct value of α.
- There is significant scatter between the curves obtained at different locations along the wall. This is particularly evident in Figs. 20(a) and 20(d), in which the pressure applied at the specimen top was adopted to represent the vertical pressure at all locations along the specimen height. This approach is clearly unacceptable and, consequently, the data in Figs. 20(a) and 20(d) have not been considered in further analyses.
- The smallest scatter is observed in tests performed with FRM (Figs. 20(e) and 20(f)). In these cases, the data generally lie between the lines corresponding to α = 0.25 and α = 0.4. According to Eq. (3), this range of α would suggest a φ' value in the range 14º - 23.5º, clearly unreasonable for sand.

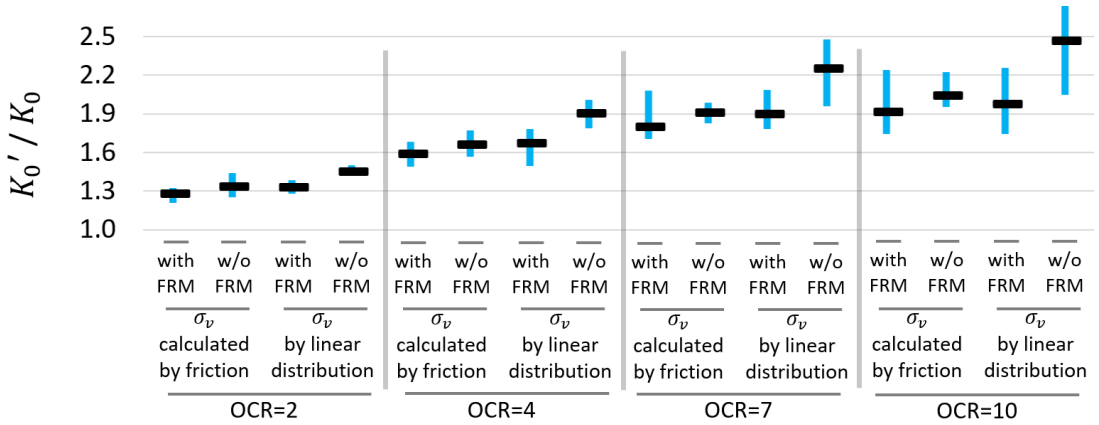

Fig. 21. Summary of K_0'/K_0 obtained for different test conditions and different assumptions

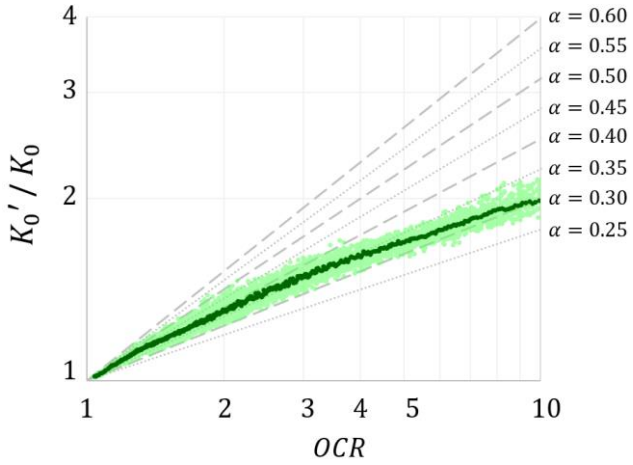

Fig. 22 Average values of K_0'/K_0 versus OCR

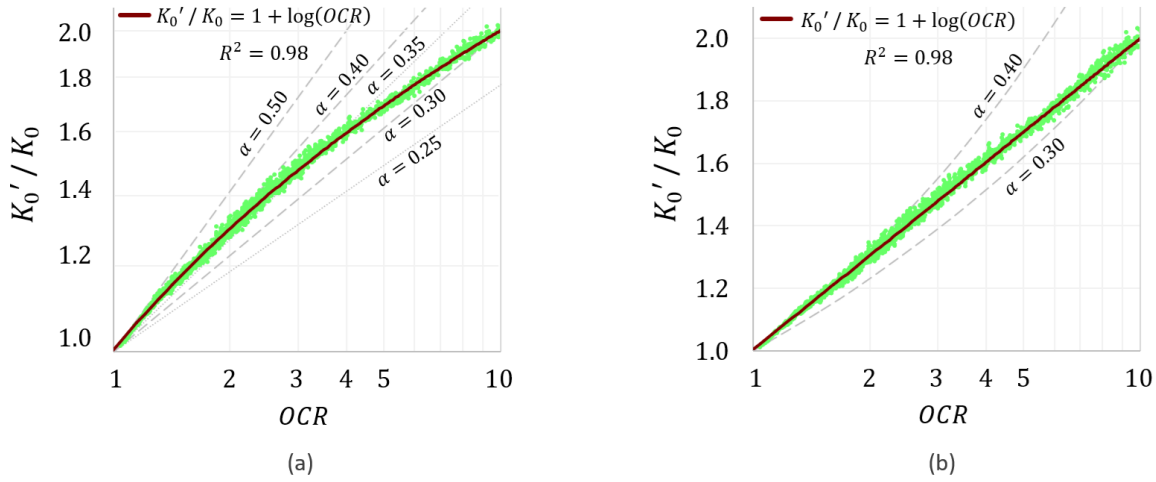

Fig. 23 K_0'/K_0 versus OCR, with fitted curve, (a) log-log plot and (b) semi-log plot

A summary of Fig. 20 is shown in Fig. 21, where the averages of K_0'/K_0 over the specimen height are shown for different values of OCR, different test conditions, and different assumptions regarding the distribution of vertical pressure.

A summary of Fig. 20 is shown in Fig. 21, where the averages of K_0'/K_0 over the specimen height are shown for different values of OCR, different test conditions, and different assumptions regarding the distribution of vertical pressure

Fig. 21 indicates that when FRM are employed, reasonably consistent values of K_0'/K_0 result based on

vertical pressure distribution obtained from both friction measurements and from an assumed linear variation of vertical pressure. The values obtained based on the linear variation are fractionally higher than those based on friction measurements. When FRM are not employed, the values based on friction measurements are compatible with those obtained with FRM. However, without FRM, the assumption of a linear variation of vertical pressure results in significantly higher values of K_0'/K_0 over the entire range of *OCR*. Consequently, a reliable estimation of K_0'/K_0 requires either use of FRM or measurement of side-wall friction; a linear distribution of vertical pressure cannot be assumed unless side-wall friction is minimized.

Overall, the most consistent values of K_0'/K_0 were obtained by estimating the vertical pressure distribution on the basis of the friction measurements, from tests both with and without FRM. Consequently, the relationship between K_0'/K_0 and *OCR* was established on the basis of these values, taking the measured horizontal pressure and the estimated vertical pressure, to estimate pairs of *OCR* and K_0'/K_0 at the location of each null gauge, continuously, during unloading. All of these pairs, from the tests both with and without FRM were tabulated in order of increasing *OCR* and, in view of the large amount of data, a moving average filter was used to plot Fig. 22 showing K_0'/K_0 as a function of *OCR*; the coarser relation was obtained with a moving average subset of 3, and the finer relation with a subset of 10.

A smooth curve is seen to result, corresponding to α varying from about 0.4 at low *OCR* to 0.3 at an *OCR* of 10, consistent with the observation presented above. A similar variation of α was observed in the tests performed on small specimens by Talesnick *et al*. (2020). The data of Fig. 22 may be represented by the following expression

$$K_0'/K_0 = 1 + C \cdot \log(OCR) \quad (4)$$

Eq. (4), with $C = 1$, provides an excellent fit to the data, at least up to an *OCR* of 10; in Fig. 23(a) the vertical axis is shown on a log scale and Fig. 23(b) on an arithmetic scale.

5. Conclusions

Laterally confined compression tests have been carried out on loose sand, measuring lateral pressure with null pressure gauges, side wall friction with newly designed friction meters and applied pressure and base pressure with load cells. The test results have demonstrated the importance of accounting for side wall friction when evaluating the distribution of vertical pressure along the height of the soil specimen, and the coefficient of lateral earth pressure at rest, K_0, during virgin loading and K_0' during unloading. Measurement of the friction distribution along the side walls, both when employing and not employing friction reduction measures (FRM) indicated relatively uniform friction during virgin loading, leading to a linear distribution of vertical pressure. Consequently, the vertical pressure, at the depths of the null pressure gauges, could be estimated from the applied pressure at the specimen top and measured pressure at the specimen base, without the need for friction measurement, simplifying the evaluation of K_0. During unloading, friction was found to be reasonably uniform when FRM were employed; however, this was not the case without FRM, and friction measurements were necessary in order to obtain a reasonable distribution of the vertical pressure and of K_0'.

From the above measurements, the coefficient of earth pressure at rest during virgin loading, K_0, was found to be in the range 0.47 – 0.54. If Eq. (1) is valid, this would indicate a φ' value in the range 32º - 27º - slightly low for this sand. Further tests, with materials of significantly different φ' values and different relative densities, are required in order to establish whether equation (1), which is theoretically incorrect, is empirically applicable. During unloading, the ratio, K_0'/K_0 was found to increase smoothly with *OCR*, but not as a linear function of OCR^{α}, with α constant and equal to sin φ', as is commonly assumed. In the present investigation, an alternative expression, $K_0'/K_0 = 1 + C \cdot \log(OCR)$, with $C = 1$, was found to provide good fit with the experimental data, at least up to an *OCR* of 10. Clearly, additional tests, on different granular materials and at varying densities, are required in order to check the general validity of an expression of this form and the significance of the parameter *C*.

References

ASTM (2000), *Standard test methods for minimum index density and unit weight of soils and calculation of relative density*. ASTM D-4254-00. West Conshohocken, PA, USA.

ASTM (2017), *Standard practice for classification of soils for engineering purposes (Unified Soil Classification System)*. ASTM D2487-17. West Conshohocken, PA, USA.

Boulfoul, K., Hammoud, F. and Abbeche, K. (2020), "Numerical study on the optimal position of a pile for stabilization purpose of a slope", *Geomech. Eng*., **21**(5), 401-411. https://doi.org/10.12989/gae.2020.21.5.401.

CGS (2006), (Canadian Geotechnical Society), *Canadian foundation engineering manual*, 4th Ed., Richmond, BC, Canada.

Dehghanbanadaki, A., Motamedi, S. and Kamarudin, A. (2020), "FEM-based modelling of stabilized fibrous peat by end-bearing cement deep mixing columns", *Geomech. Eng*., **20**(1), 75-86. https://doi.org/10.12989/gae.2020.20.1.075.

Frydman, S. (2000), "Shear strength of Israeli soils", *Isr. J. Earth Sci*., **49**(2), 55-64.

Gao, Y. and Wang, Y.H. (2014), "Experimental and DEM examination of K_0 in sand under different loading conditions", *J. Geotech. Geoenviron. Eng*., **140**(5). https://doi.org/10.1061/(ASCE)GT.1943-5606.0001095.

Golpasand, M.R.B., Do, N.A., Dias, D. and Nikudel, M.R. (2018), "Effect of the lateral earth pressure coefficient on settlements during mechanized tunneling", *Geomech. Eng*., **16**(6), 643-654. https://doi.org/10.12989/gae.2018.16.6.643.

Gu, X., Hu, J. and Huang, M. (2015), "K_0 of granular soils: a particulate approach", *Granular Matter*., https://doi.org/10.1007/s10035-015-0588-7.

Gu, X., Hu, J., Huang, M. and Yang, J. (2018), "Discrete element analysis of the K_0 of granular soil and its relation to small strain shear stiffness", *Int. J. Geomech. – ASCE*, **18**(3). DOI: https://doi.org/10.1061/(ASCE)GM.1943-5622.0001102.

Hossain, A.M. and Andrus, R.D. (2016), "At-rest lateral stress coefficient in sands from common field methods", *J. Geotech.*

Geoenviron. Eng., **142**(12). https://doi.org/10.1061/(ASCE)GT.1943-5606.0001560.
ISI (Israel Standards Institute) (2000), *Israel Standard 940, Part 1: Geotechnical design: Geotechnics and foundations for civil engineering*. Tel Aviv, Israel.
Jaky, J. (1944), "The coefficient of earth pressure at rest", *J. Soc. Hung. Archit. Engrs*., **78**(22), 355-358 (in Hungarian).
Mansouri, H. and Asghari-Kaljahi, E. (2019), "Two dimensional finite element modeling of Tabriz metro underground station L2-S17 in the marly layers", *Geomech. Eng*., **19**(4), 315-327. https://doi.org/10.12989/gae.2019.19.4.315.
Mayne, P.W. and Kulhawy, F.H. (1982), "K_0–*OCR* relationships in soil", *J. Geotech. Div. – ASCE*, **108**(6), 851-872.
Michalowski, R.L. (2005), "Coefficient of earth pressure at rest", *J. Geotech. Geoenviron. Eng*., **131**(11), 1429-1433.
Schmidt, B. (1966), Discussion of 'Earth pressures at rest related to stress history' (Brooker & Ireland, 1965), *Can. Geotech. J*., **3**(4), 239-242.
Talesnick, M. (2005), "Measuring soil contact pressure on a solid boundary and quantifying soil arching", *Geotech. Test. J. ASTM*, **28**(2), 171-179.
Talesnick, M. (2012), "A different approach and result to the measurement of K_0 of granular soils", *Géotechnique*, **62**(11), 1041-1045. https://doi.org/10.1680/geot.11.P.009.
Talesnick, M., Ringel, M. and Avraham, R. (2014), "Measurement of contact soil pressure in physical modeling of soil–structure interaction", *Int. J. Phys. Model. Geotech*., **14**(1), 3-12, https://doi.org/10.1680/ijpmg.13.00008.
Talesnick, M. and Frydman, S. (2019), "Pathology of a research error: Coefficient of earth pressure at-rest for cohesionless soils", *Proceedings of the 72nd Annual Conference of the Canadian Geotechnical Society, GeoSt.John's 2019*, St John's NFLD, Canada, October.
Talesnick, M. and Ringel, M. (2020), "Development of a soil boundary friction meter: application to scale model testing", *Int. J. Phys. Model. Geotech*., **22**(1), 26-37. https://doi-org /10.1680/jphmg.20.00019.
Talesnick, M., Nachum, S. and Frydman, S. (2020), " K_0 determination using improved experimental technique", *Geotechnique*, https://doi.org/10.1680/jgeot.19.P.019.
Talesnick, M. and Bolton, M.D. (2020), "Effect of structural boundaries and stress history on at-rest soil pressure of sand", *Int. J. Phys. Model. Geotech*., **21**(4), 1-10. https://doi.org/10.1680/jphmg.19.00049.
Tognon, A.R., Rowe, R.K. and Brachman, R.W.I. (1999), "Evaluation of side wall friction for a buried pipe testing facility", *Geotext. Geomembranes*, **17**(4), 193-212. https://doi.org/10.1016/S0266-1144(99)00004-7.
Watcharasawe, K., Jongpradist, P., Kitiyodom, P. and Matsumoto, T. (2021), "Measurement and analysis of load sharing between piles and raft in a pile foundation in clay", *Geomech. Eng*., **24**(6), 559-572. https://doi.org/10.12989/gae.2021.24.6.559.
Yazici, M.F. and Keskin, S.N. (2021), "Optimum design of multi-anchored Larssen type sheet pipe wall for temporary construction works", *Geomech. Eng.*, **27**(1), 1-11. https://doi.org/10.12989/gae.2021.27.1.001.
Zheng, J., Li, L. and Daviault, M. (2021), "Experimental study of the effectiveness of lubricants in reducing sidewall friction", *Int. J. Geomech. – ASCE*, **21**(5), https://doi.org/10.1061/(ASCE)GM.1943-5622.0002003.